

Ore-waste and ore type classification using portable XRF: a case study of an iron mine from the Quadrilátero Ferrífero, Brazil

*Classificação de minério-estéril e tipo de minério utilizando FRX Portátil:
um estudo de caso de uma mina de ferro do Quadrilátero Ferrífero, Brasil*

Emílio Evo Magro Corrêa Urbano¹ , João Felipe Coimbra Leite Costa² ,
Leonardo Martins Graça¹ , Ricardo Augusto Cipriano Scholz¹ 

¹Universidade Federal de Ouro Preto - UFOP, Departamento de Geologia, Campus Morro do Cruzeiro, s/n, Bauxita, CEP 35400-000, Ouro Preto, MG, BR (emilioevourbano@gmail.com; leonardo.graca@ufop.edu.br; ricardo.scholz@ufop.edu.br)

²Universidade Federal do Rio Grande do Sul - UFRGS, Departamento de Engenharia de Minas, Porto Alegre, RS, BR (jfelipe@ufrgs.br)

Received on September 19th, 2019; accepted on April 9th, 2020

Abstract

Grade control is a fundamental activity for Short-Term Mine Planning as it validates the ore-waste and ore type classification of mine faces. Geological mapping and quasi-mining sampling provide indispensable information for the Short-Term Mine Planning team to update block models and for grade control of the run-of-mine (ROM). However, laboratory turnaround can take too long and not be timely for operational needs, affecting mining efficiency. To propose a solution for this issue we tested the accuracy of portable X-Ray Fluorescence (XRF) for ore-waste and ore type classification according to iron and phosphorus grade. Thus, iron ore run-of-mine samples from the Quadrilátero Ferrífero were analyzed with the portable XRF as pressed pellets. As a result, the overall accuracy of ore-waste classification was above 92% for different cut-off grades. On the other hand, while ore type classification had a better accuracy without calibration factors for iron, the use of calibration factors significantly improved the accuracy of ore type classification for phosphorus. Therefore, despite the portable XRF presenting good accuracy for ore-waste and ore type classification, further developments are still necessary on automatic information processing systems and sample support validation so that this analytical tool can be used on a large scale by grade control teams. Finally, the combined use of portable XRF and other techniques, such as Hyperspectral Sensing or XRD, can be of great value for mine operations.

Keywords: Grade control; Mining; X-ray fluorescence; Iron ore; Mine planning.

Resumo

O controle de qualidade é uma atividade fundamental para o Planejamento de Lavra de Curto Prazo, pois valida a classificação de minério-estéril e tipo de minério nas frentes de lavra. O mapeamento geológico e a amostragem de grande volume fornecem informações indispensáveis para a equipe de Planejamento de Mina de Curto Prazo atualizar os modelos de blocos e fazer o controle de qualidade do *run-of-mine*. No entanto, a resposta do laboratório pode levar muito tempo e não ser oportuna para as necessidades operacionais, afetando a eficiência da mineração. Para propor uma solução para esse problema, testamos a acurácia da espectrometria por Fluorescência de Raios X (FRX) portátil para classificação de minério-estéril e tipos de minério de acordo com o teor de ferro e fósforo. Assim, amostras de minério de ferro do Quadrilátero Ferrífero foram analisadas pela FRX portátil como pastilhas prensadas. Como resultado, a acurácia geral da classificação de minério-estéril foi superior a 92% para diferentes teores de corte. Por outro lado, enquanto a classificação dos diferentes tipos de minério teve uma melhor acurácia sem fatores de calibração para o ferro, o uso destes fatores melhorou significativamente a acurácia da classificação do tipo de minério em relação ao fósforo. Portanto, apesar da FRX portátil apresentar boa acurácia para o controle de qualidade, ainda são necessários mais avanços em relação a sistemas automatizados de processamento de informações e validação do suporte amostral para que esta ferramenta possa ser usada em larga escala pelas equipes de controle de qualidade. Finalmente, o uso combinado da FRX portátil e outras técnicas, como análise por Imagens Hiperespectrais ou Difractometria de Raios-X (DRX), pode ser de grande valia para as operações das minas.

Palavras-chave: Controle de qualidade; Mineração; Fluorescência por raios X; Minério de Ferro; Planejamento de mina

INTRODUCTION

Mining follows a sequence of planned activities defined by long- and short-term planning. In long-term planning, the deposit is divided into a block model with grades estimated from data usually obtained by diamond drill holes (Figure 1A). Every year, part of the deposit is selected to be mined. In turn, the Short-Term Planning team provides more detailed geological mapping and sampling as new ore is exposed, helping to reduce uncertainty about block grades (Costa et al., 2001; Araújo et al., 2018).

Thus, geological mapping and quasi-mining sampling are of paramount importance for short-term planning, as they are used to update block models previously estimated with Long-Term Planning data (Figure 1B). These samples also provide information for the grade control team in order to plan ore blend and reach the quality specifications for run-of-mine (ROM), maximizing the net present value, while minimizing deviations from desired production targets (Blom et al., 2019). For this procedure, it is necessary to obtain representative samples and use appropriate analytical protocols in the laboratory (Spangenberg and Minnitt, 2014).

The time required to obtain the chemical results is of fundamental importance for updating block models, guaranteeing correct mining (*e.g.*, waste to the waste dump and ore to a processing plant), adequate fleet allocation, and production rate. In some cases, the laboratory turnaround can be on the order of days due to the distance from the mine site or other reasons (Figure 1C). To propose a solution for this timing issue, we investigate the application of portable X-Ray Fluorescence (XRF) on ore-waste and ore type classification for iron ores, according to iron and phosphorus contents.

Different studies have been published related to the use of portable XRF in the mining industry. Gazley et al. (2014) presented how inconsistencies related to multiple geologists logging in a gold mine were solved by the development of an objective logging method based on portable XRF data. In another case study, the incorporation of portable XRF data in geological modeling improved its confidence level, as it allowed for better management of milling processes through the development of metallurgical proxies (Gazley et al., 2015).

In recent years, studies have been developed based on the application of different types of portable XRF for in-pit

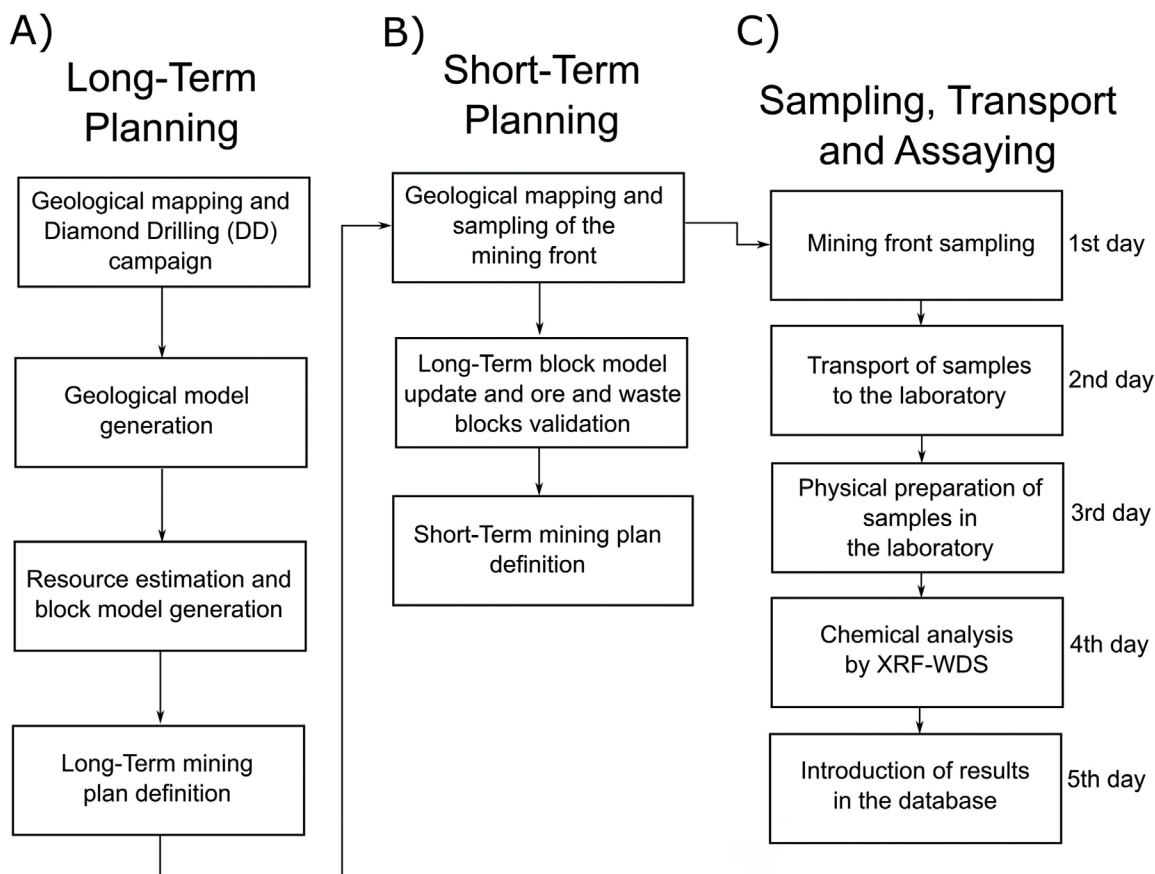


Figure 1. Workflow of (A) Long-Term Planning, (B) Short-Term Planning and (C) the processes related to sampling and assaying.

grade control and ore-waste classification. Nayak et al. (2017) proposed the use of shovel based XRF sensors for selective partitioning of ore blocks, improving ore-waste discrimination and reducing processing costs by identifying and omitting material below the cut-off grade. Hawke and Bachmann (2018) presented a new XRF tool for blasthole logging. This tool aims at separating different sections of a hole based on its chemical composition, providing more detailed grade control and supporting selective mining.

The new approaches proposed here do not seek to match the accuracy of the portable XRF with conventional laboratory techniques, but to generate appropriate information for ore-waste separation and grade control. Therefore, portable XRF analyses of iron ore samples are compared to the laboratory results and discussed according to the cut-off grade and ore type classification.

GEOLOGICAL SETTING

The Quadrilátero Ferrífero (QFe) is a mineral province located on the southeastern border of the São Francisco Craton and comprises Archean metamorphic complexes consisting of gneisses, migmatites and granitoids, an Archean sedimentary sequence (Rio das Velhas Supergroup), and a Paleoproterozoic sedimentary sequence (Minas Supergroup) (Figure 2). The latter is composed by phyllites, quartzites, metaconglomerates, banded iron formations, and dolomites. This region went

through two orogenic events, the Transamazonian orogeny at 2.1–2.0 Ga and the Brasiliano orogeny at 0.65–0.50 Ga (Alkmin and Marshak, 1998; Farina et al., 2016). This led to a complex deformation pattern and metamorphism that varies between greenschist in the east to amphibolite facies in the west. Itabirite is the metamorphosed equivalent of the banded iron formations and is found in a variety of compositions, including quartz itabirite, dolomitic itabirite, and amphibolitic itabirite (Rosière et al., 2008).

The formation of high-grade iron deposits is related to a combination of hypogene and supergene processes. High-grade ore bodies are found mainly in sites of low strain rates, such as large fold hinges, and faults worked as conduits for mineralizing fluids (Rosière et al., 2008). In most of the iron deposits of the QFe, the ore minerals are hematite, magnetite, and goethite, and the main gangue minerals are quartz, kaolinite, and gibbsite. More rarely, carbonates, chlorite, amphibole, and biotite may also occur (Fernandes, 2008; Ortiz, 2014).

The mine sampled for this study is located on the eastern limb of the Moeda Syncline, which is overturned. This deposit comprises discontinuous lenses of hematite with diversified geometries and dimensions that grade laterally and with depth to quartz-rich itabirites (Fernandes, 2008). In this mine, the itabirites are subdivided according to their composition and degree of compactness. The most common ore type is quartz itabirite and, when significantly enriched in iron, it is referred to simply as hematite.

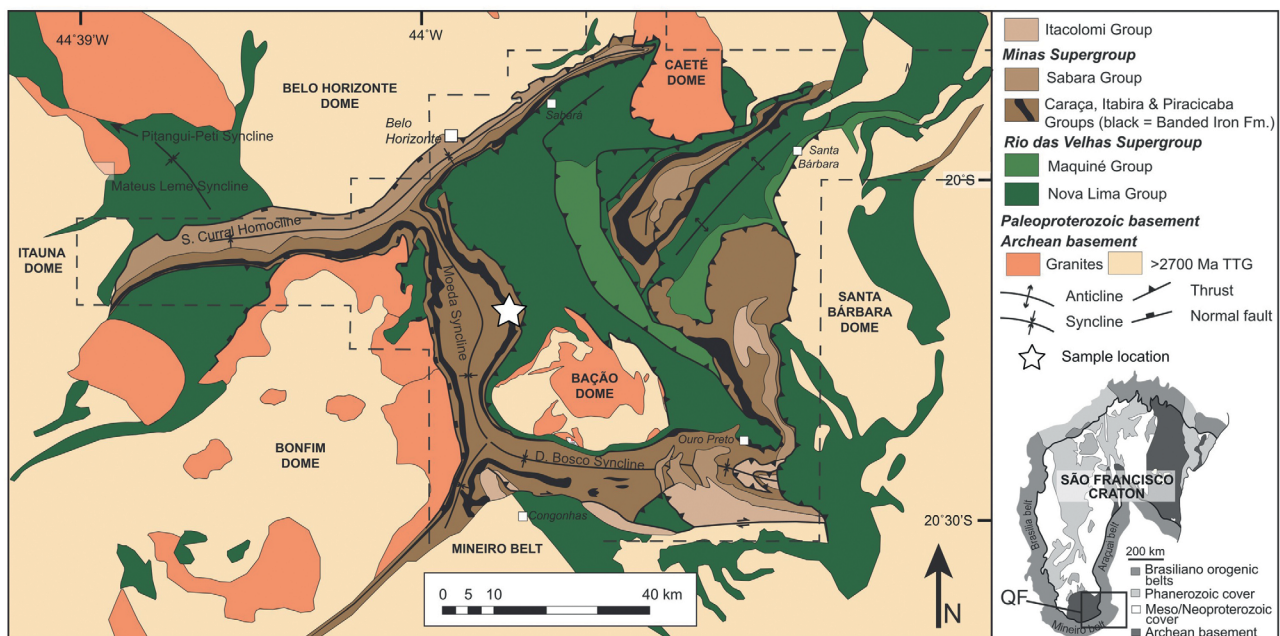


Figure 2. Geological map of the QFe showing the main stratigraphic units, structures and samples location (modified after Farina et al., 2016).

MATERIALS AND METHODS

Twenty-five samples of itabirites were analyzed with a portable XRF and compared to the analysis performed by XRF-wave dispersive spectrometry (XRF-WDS) at the mine laboratory to evaluate the accuracy of ore-waste and ore type classification of the former. Samples provided by Vale S.A. are from a mine located in the western part of the QFe, Brazil, and collected during a Reverse Circulation (RC) drilling campaign. The portable XRF used was a Vanta™ (VMR), M Series, with a workstation, both from Olympus. It is equipped with a silicon drift detector (SDD) and a 50 kV X-ray tube with Rhodium (Rh) anode.

All the samples were crushed and sieved below 1 mm and made into pressed pellets using the REFLEX Portable Press (Figure 3A). Then, the analyses were performed on the pressed pellets for one minute. The influence of the analysis duration on the results was evaluated by analyzing Certified Reference Materials (CRM) for 30, 60, 90, and 120 seconds. As part of the Quality Assurance-Quality Control (QA-QC) protocol, a blank sample was tested at the beginning of the session and, if the result was acceptable, a batch of five samples followed by CRM, blank and duplicate were analyzed (Figure 3B). CRM 010, 019, and 026

used in this study are all from the QFe region and were produced by the company ITAK. The methodology of Stanley and Lawie (2007) was used to calculate the coefficient of variation, a parameter that allows to evaluate the quality of sample preparation.

Initially, the tests were performed without calibration factors. However, once the initial results were available, calibration factors were calculated for iron and phosphorus using the traditional regression equation, a first-order polynomial equation. Then, these factors were applied to the initial results and compared to the cut-off grade and ore type classification (Figure 3C).

We evaluated the influence of different cut-off grades on the accuracy of ore-waste classification for each calibration strategy, in order to evaluate the efficiency of the use of the portable XRF for this task. The use of the portable XRF for grade control was tested using an ore classification system based on the iron and phosphorus content (Table 1). This system classifies the ore into ten types, which are related to the grade zones of each element. The codes related to each ore type were created so that these data could be correlated on the graphs presented later in this paper. Regarding the contaminants, phosphorus monitoring is critical as this deleterious element must only be present in low grades in the

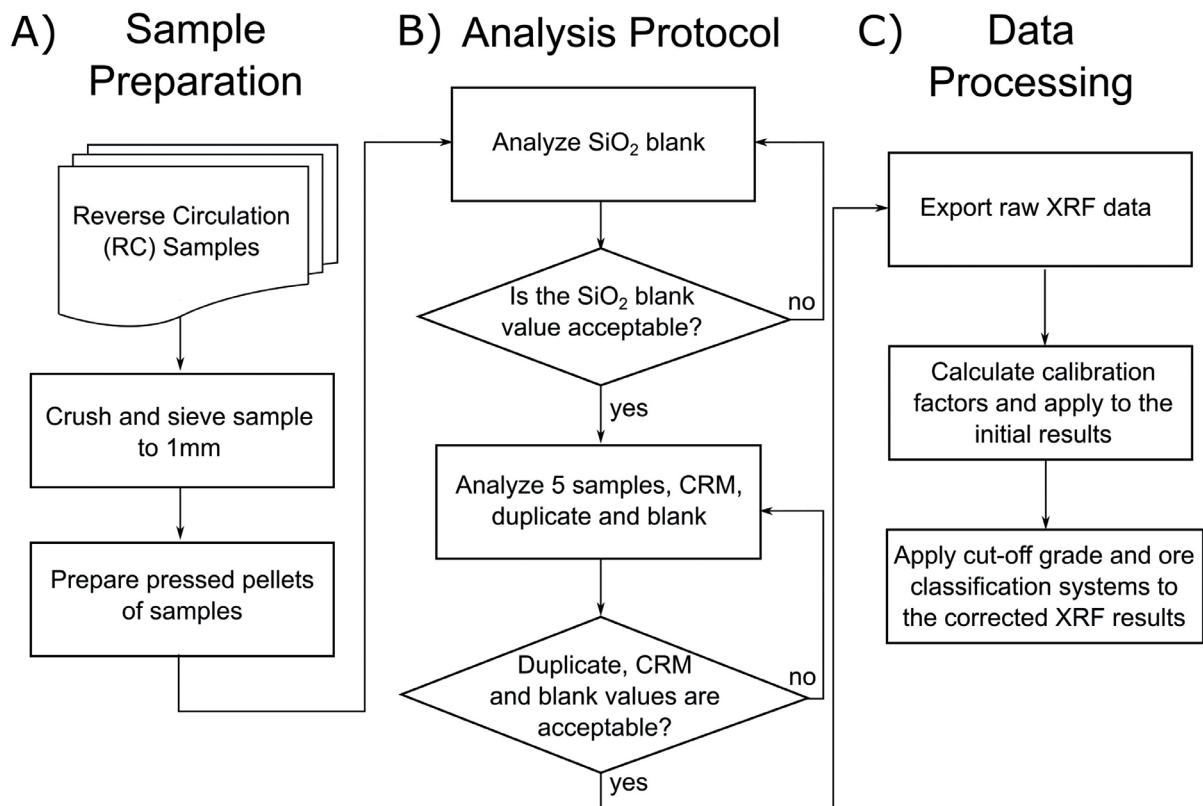


Figure 3. Workflow diagram of (A) sample preparation, (B) analysis protocol and data processing of portable X-ray fluorescence results for ore-waste and (C) ore type classification of itabirites.

ROM (< 0.05%). Also, concentration processes are not very efficient at removing it from iron ore, thus, requiring rigid control on the presence of this element during mining (Pereira and Papini, 2015).

RESULTS

First, data related to the calculation of calibration factors, sample preparation, and analytical time tests are presented to demonstrate that the bias related to the analyses is acceptable for the objective of this study. Then, the portable XRF results are presented for ore-waste and ore type classification, as proposed. The analytical results (Laboratory and portable XRF) and ore type classification of each sample are presented in Appendix 1.

Calibration factors

Calibration factors were calculated for iron and phosphorus using a regression equation based on the comparison of the results from the portable XRF and the Laboratory XRF. All data obtained were considered for the calculation of the calibration factor for phosphorus, since none of the samples presented concentrations below the limit of

detection indicated by the manufacturer (0.005%). Also, all the analyses conducted with the portable XRF used in the dataset reached the full counting time required for precise measurement. Figure 4 illustrates the correlation between the Laboratory and portable XRF results. To help with comparison, the 1:1 line is also presented.

The slope of the regression line and the coefficient of determination (R^2) indicate, respectively, good accuracy and fit for the iron results ($R^2 = 0.9951$), whereas the phosphorus results are less accurate ($R^2 = 0.8708$).

Regarding the iron content, the portable XRF analysis confirmed it, both for low and high values, around 20 and 65%. Although the Phosphorus coefficient of determination was lower, it can also be considered a good result, since portable XRF analysis confirmed similar maximum and minimum results.

Duplicates samples

The results for iron and phosphorus for five duplicate samples demonstrate the quality of sample preparation. The results for iron show relative difference of less than 5% between the primary and duplicate samples, which is a good result for a major element (Figure 5A). The mean coefficient of variation (CV) for iron is 1.19%.

Table 1. Classification system of different iron ore types according to iron (Fe) and phosphorus (P) grade.

Ore Classification System					
Fe	(%)	Code	P	(%)	Code
Very high	> 60	1	Very low	$P < 0.050$	6
High	$50 < Fe < 60$	2	Low	$0.050 < P < 0.100$	7
Intermediate	$40 < Fe < 50$	3	Intermediate	$0.100 < P < 0.150$	8
Low	$30 < Fe < 40$	4	High	$0.150 < P < 0.200$	9
Very Low	< 30	5	Very high	$P > 0.200$	10

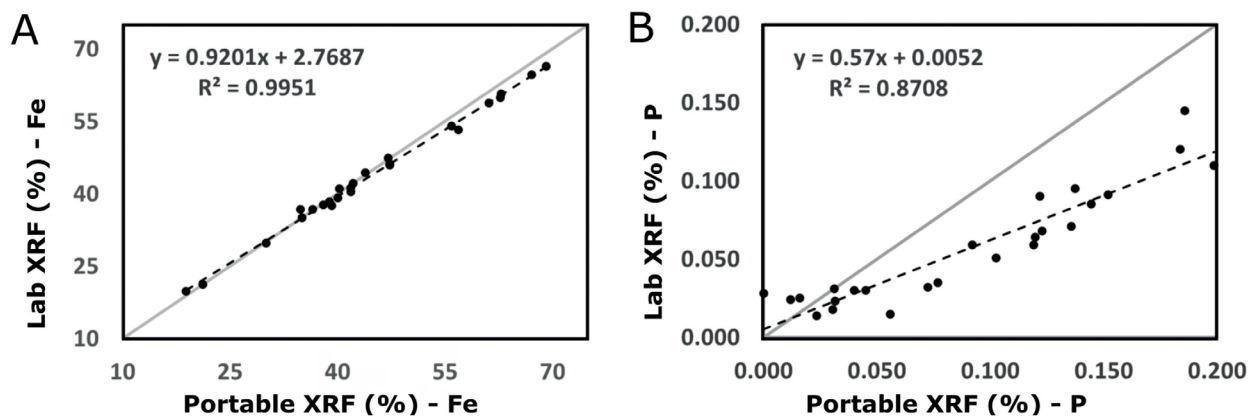


Figure 4. Comparison of Laboratory X-ray fluorescence (XRF) and portable XRF results for (A) Iron and (B) Phosphorus.

For phosphorus, the difference between the primary and duplicate samples is less than 10%, except for one sample which is slightly higher (Figure 5B). Although these results are statistically less robust than those for iron (CV = 8.47%), this is appropriate for minor elements such as Phosphorus. In this case, larger relative differences represent smaller absolute differences when compared to major elements.

The dashed line present in both graphs in Figure 5 represents relative differences of 5 and 10% for iron and phosphorus, respectively. The cone shape of the dashed lines in Figure 5B is due to its closeness to the origin of the graph.

Analytical time tests

Analytical time was important to test in order to find a balance between accuracy and productivity, so 30, 60, 90, and 120 seconds were tested (Figure 6). Thus, the differences

found for the results are relatively low: the mean CV of the three CRM is 0.56% for iron and 2.06% for phosphorus. This indicates close values for the different analytical times of the same CRM or, in other words, adequate precision.

Ore-waste classification and cut-off grade

Ore-waste definition depends on many technical factors, including grade contaminants, grindability, mineral liberation and mass recovery at the processing plant. However, in this study, we restricted ore-waste and ore type classification to iron and phosphorus cut-off grades. Therefore, we evaluated the total number of samples classified as ore by the portable XRF for variable cut-off grades and compared them to the results from the laboratory. A straightforward observation is that ore-waste classification accuracy will vary depending on the calibration strategy applied to the portable XRF and on the cut-off

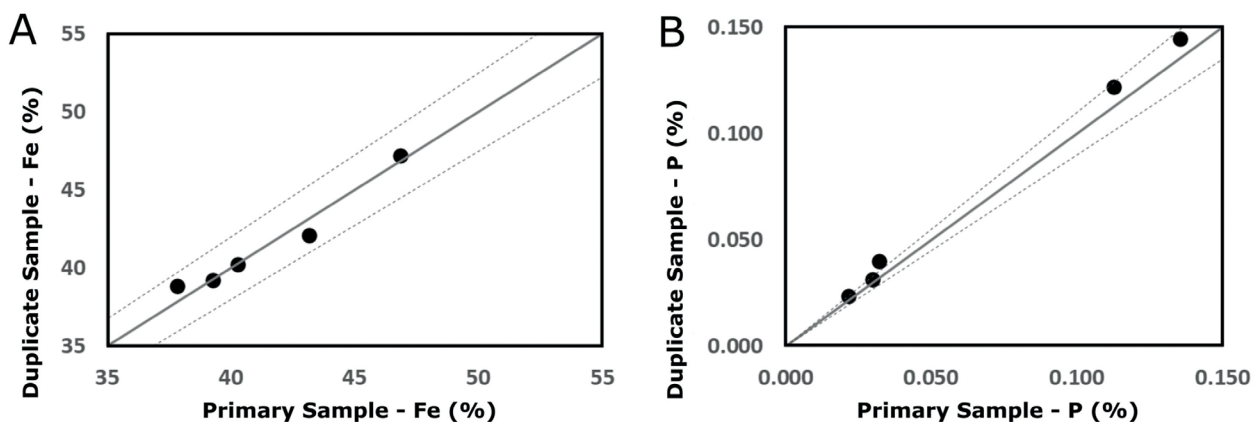


Figure 5. Duplicate results for (A) Iron and (B) Phosphorus, the dashed lines indicate an error of $\pm 5\%$ for Iron and $\pm 10\%$ for Phosphorus. Analysis was performed by portable X-ray fluorescence.

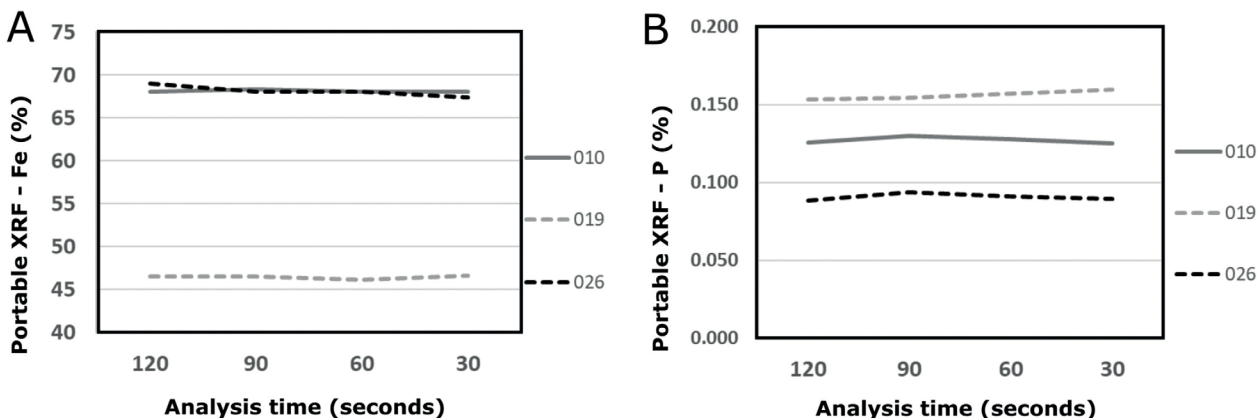


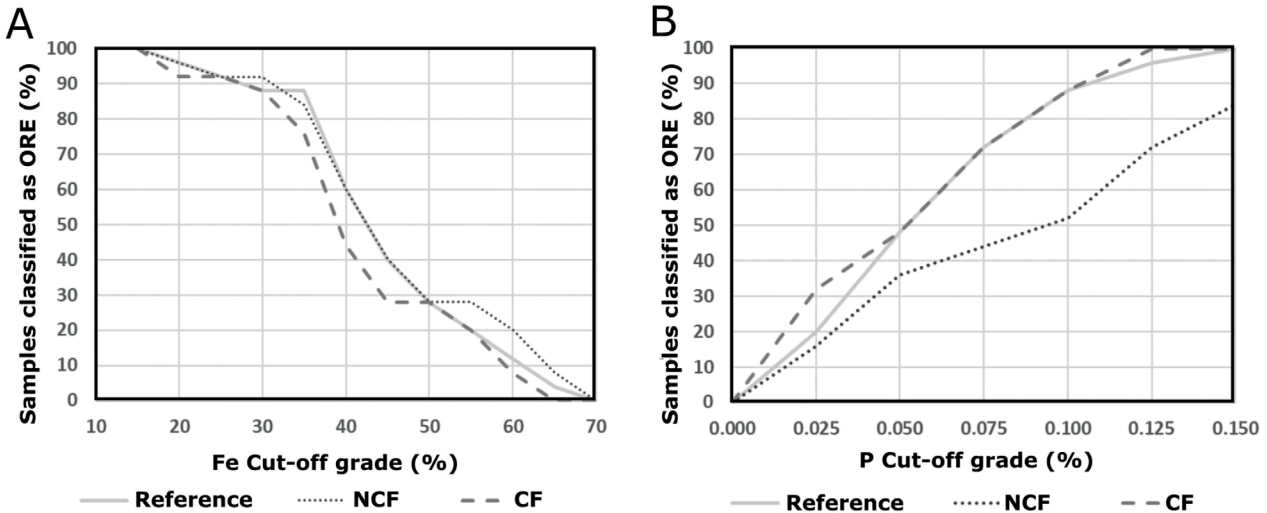
Figure 6. Analytical time tests for (A) iron and (B) phosphorus with different Certified Reference Materials (010; 019; 026).

grade (Figure 7). In this graphic, the reference curve was built with lab results while the other curves were built with results from the portable XRF using different calibration strategies.

The accuracy of the portable XRF is related to the degree of similarity of its curves with the reference curve. Total accuracy (100% of correctness) is reached when the

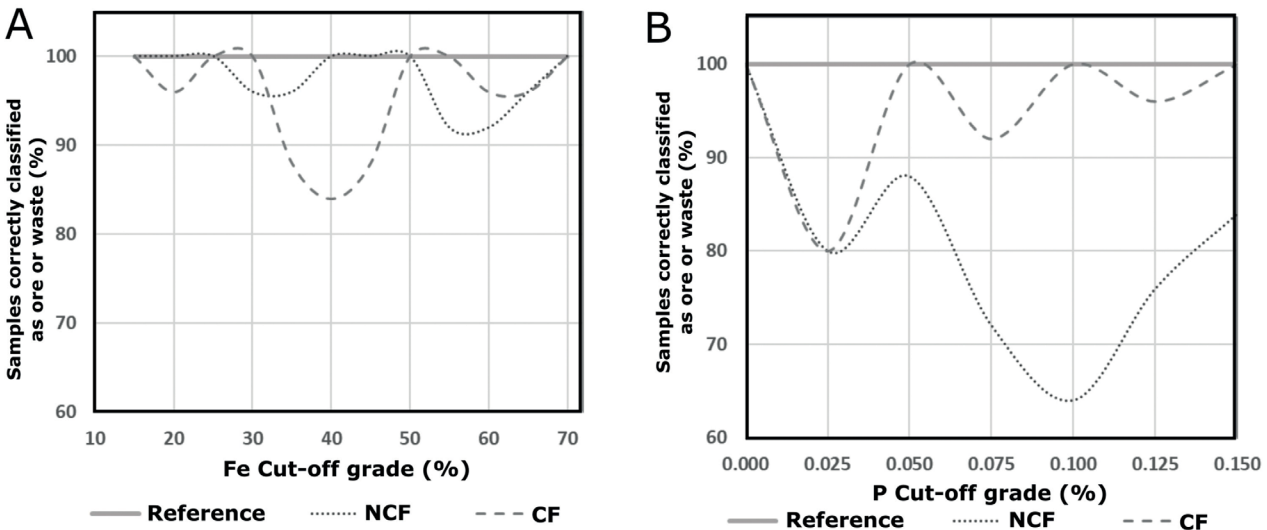
portable XRF and the reference curves overlap. A second graphic shows the number of samples correctly classified as ore or waste according to the cut-off grade and the impact of calibration strategy (Figure 8).

The two calibration strategies used present different levels of accuracy depending on the grade zone of



NCF: no calibration factor; CF: calibration factor.
Source: Modified after Araújo et al. (2018).

Figure 7. Total number of samples classified as ore according to the cut-off grade of (A) Iron and (B) Phosphorus. The reference curve was built with the results from the laboratory while the other curves represent the results from the portable X-ray fluorescence (XRF) using different calibration strategies. The accuracy of the portable XRF is related to the closeness of its curves to the reference curve.



NCF: no calibration factor; CF: calibration factor.

Figure 8. Samples correctly classified as ore or waste according to the cut-off grade for (A) iron and (B) phosphorus. The reference curve was built with the laboratory results whereas the others were created using the results of the portable X-ray fluorescence with different calibration strategies.

iron (Figures 7A and 8A). For cut-off grades below 50% for iron, the results with no calibration factor (NCF) are better adjusted to the reference curve, although there are local variations. Conversely, for cut-off grades ranging from 50 to 58% of iron, the calibration factor (CF) curve presented the best fit, while from 58 to 70% of iron, NCF and CF curves had similar accuracy, although neither was totally accurate.

For the phosphorus results, the CF curve had the best accuracy for cut-off grades ranging from 0.050 to 0.100% (Figure 7B), reaching total accuracy at the limits of this grade zone (Figure 8B). The CF curve still had the best accuracy for cut-off grades below 0.050 and above 0.100%, though it was not totally accurate (Figure 8B).

Therefore, the accuracy of the portable XRF for ore-waste classification ranges from 96 to 100% for iron and from 92 to 100% for phosphorus, depending on the cut-off grade and the calibration strategy (Table 2). However, the mean accuracy is 98.91% for iron and 97.33% for phosphorus for this set of samples (Table 2).

Ore type classification

Grade control is extremely important to guarantee that quality specifications for the ROM are met. It provides information

Table 2. Accuracy of ore-waste classification according to the cut-off grade and calibration strategy of the portable X-ray fluorescence for Iron and Phosphorus.

Cut-off grade	Calibration strategy with best accuracy	Accuracy (%)	Samples classified as ore			
			Reference	NCF	CF	
Fe (%)	15	NCF; CF	100	25	25	25
	20	NCF	100	24	24	23
	25	NCF; CF	100	23	23	23
	30	CF	100	22	23	22
	35	NCF	96	22	21	19
	40	NCF	100	15	15	11
	45	NCF	100	10	10	7
	50	NCF; CF	100	7	7	7
	55	CF	100	5	7	5
	60	CF	96	3	5	2
65	NCF; CF	96	1	2	0	
Mean accuracy		98.91				
P (%)	0.025	NCF	96	5	4	8
	0.05	CF	100	12	9	12
	0.075	CF	92	18	11	16
	0.1	CF	100	22	13	22
	0.125	CF	96	24	18	25
	0.15	CF	100	25	21	25
	Mean accuracy		97.33			

NCF: no calibration factor; CF: calibration factor.

required to plan ore blends with different grades of iron and contaminants in order to maximize reserves and production. The ore type classification system used with the portable XRF results is depicted in Table 1.

Initially, all samples were analyzed with NCF and three samples were misclassified according to the iron grade (Figure 9A). Then, calibration factors were calculated with linear regression equations and applied to the initial results. This worsened the classification of the samples when compared to the initial results, with five samples being misclassified (Figure 9B). These results correspond to an accuracy for ore type classification of 88 and 80% for each calibration strategy, respectively.

For phosphorus, the analyses with NCF had worse results, with fifteen ore samples being misclassified (Figure 9C). In contrast, the ore type classification using the CF reached total accuracy (Figure 9D). The accuracy of these results corresponds to 40 and 100%, respectively.

DISCUSSION

Correct rock destination is extremely relevant for the profitability of mine operations as ore processing and hauling are the most cost-intensive stages of a mining cycle (Lessard et al., 2014). The development of cheaper and more advanced sensors in the last few decades provides an opportunity for real-time monitoring of the ROM. This monitoring may be used to detect material heterogeneity in the pit and to sort the ore according to its composition, reducing processing costs, as less material below the cut-off grade is transported to the mineral processing plant (Nayak et al., 2017). Thus, portable XRF may be a powerful tool for effective and real-time grade control of the ROM. In the following part of this study, we will discuss the fitness of portable XRF data for this task, consider the possible sampling methods, and theoretically compare it to other analytical techniques.

Ore-waste and ore type classification accuracy

According to the results, the use of the portable XRF for ore-waste classification according to iron grade could have caused a loss of production of 4% for this group of samples in the worst case scenario (96% of accuracy for cut-offs of 35, 60 and 65% of iron). It means that one block of ore, out of a total of 25, would not be transported to the processing plant. On the other hand, in the best scenario, all blocks would be transported to the correct destination. In the case of phosphorus, the situation would be very similar. In the worst case scenario, the loss of production would be of 8% (92% of accuracy for a cut-off of 0.075% of phosphorus), or two ore blocks would not be mined as planned and, in the best scenario, all blocks would be hauled to the correct destination.

Regarding the classification of the different ore types according to the iron grade, the accuracy did not improve after using the calibration factor, as five samples were misclassified instead of three (Figure 9). On the other hand, the application of CF in the phosphorus results made a significant improvement, since all the samples were correctly classified. It indicates that different types of ores could be successfully blended in order to approach the chemical composition desired for production.

A possible reason for this difference in accuracy is that phosphorus has characteristic X-rays with much less energy ($K_{\alpha} = 2.01$ keV and $K_{\beta} = 2.14$ keV) than those of Iron ($K_{\alpha} = 6.4$ keV and $K_{\beta} = 7.06$ keV) due to its lower atomic

mass. This makes it much harder to quantify phosphorus and other light elements, hence the need to use CFs.

Note that the accuracy of the ore type classification will also depend on the grade range defining the classes (rock type). The larger the grade range of each ore type, the greater the accuracy achieved in its classification.

Sample support for grade control

Another important matter for the use of portable XRF is sample support. In the iron ore mines at QFe, it is common practice to sample trenches dug with excavators on the mine faces. These quasi-mining samples are usually

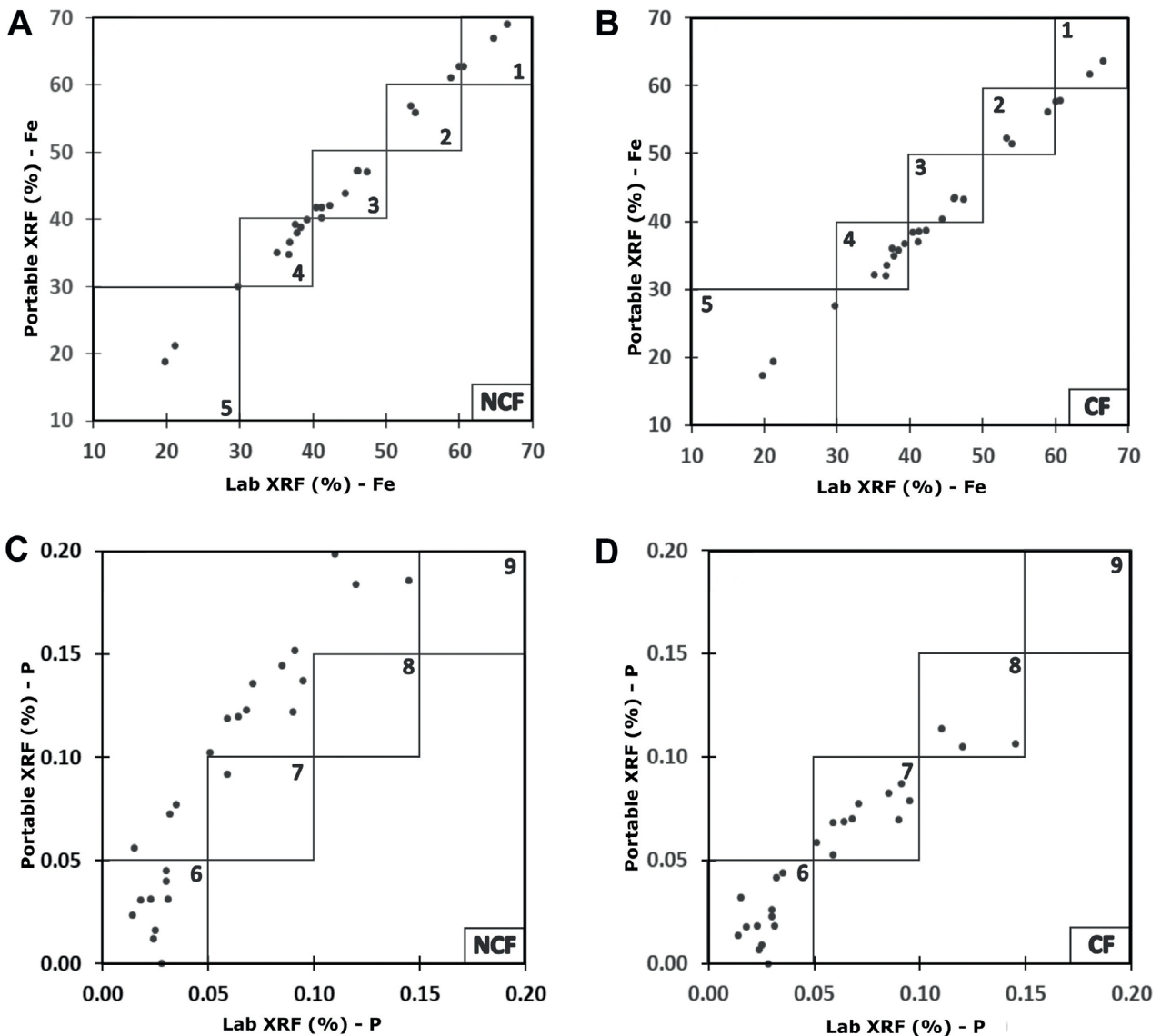


Figure 9. Classification plots for different ore types based on (A and B) iron and (C and D) phosphorus grades. The numbers indicate the ore codes of Table 1. Samples correctly classified must fall inside the squares.

partly composed of coarse fragments which would need to be crushed and ground in the lab to make pressed pellets, then analyzed by portable XRF. This would be very time-consuming. Alternatively, samples from blast holes present three advantages:

- sample density is high due to relative closeness between the blast holes;
- preparation time is shorter because samples are already ground;
- there are no additional costs associated with sampling, as the blast hole must be drilled anyway.

However, sampling blast holes have some technical challenges that must be considered, such as the bias caused by density and particle size segregation (Snowden, 1993). It has been demonstrated that this sampling technique can be fit-for-purpose for grade control of open-pit iron ore mines, but it is necessary to validate the method for each mine due to deposit heterogeneity (Engström and Esbensen, 2017).

Portable XRF versus other analytical techniques

In the last few decades, some studies tested the application of Hyperspectral Sensing for mineral mapping of mine faces (Fraser et al., 2006; Ramanaidou and Wells, 2011; Dalm et al., 2017). Although it successfully determined areas rich in kaolinite, hematite, and goethite, this technique cannot determine the presence of deleterious elements (Si, Al or P) in the structure of goethite. Another knowledge gap is whether hyperspectral cameras have the ability to detect and quantify phosphates below 0.5% in iron ore mine faces. Additionally, mine faces must be clean of dust or ex situ particles in order to be analyzed by Hyperspectral Sensing.

Regarding the use of X-Ray Diffractometry (XRD) for grade control of iron ores, it presents similar possibilities and limitations as Hyperspectral Sensing. Although it provides semi-quantitative mineralogical analysis, it has a limit of detection of approximately 0.5% and it is not possible to determine mineral chemistry without the support of other techniques (Parian et al., 2015; Andrade et al., 2016; Urbano, 2017).

More recently, digital images of unmanned aerial vehicles have been tested for automated lithological classification (Beretta et al., 2019). In this case study, RGB color channels were used to classify the lithology according to its known colors through the application of Machine Learning algorithms, reaching an accuracy greater than 90%. On the other hand, the success of this technique for the discrimination of iron ore and waste according to phosphorus content may not be effective because the presence of phosphorous does not typically change the color of the rock. Mine faces

must also be clean of transported particles so they can be correctly analyzed. Nevertheless, tests are necessary to evaluate the efficiency of this application.

Thus, as far as the results presented in this study have demonstrated, portable XRF can be a powerful tool for grade control in iron ore mines, especially those that contain zones with high phosphorous contents. Moreover, the use of this technology together with other analytical techniques that detect minerals, such as Hyperspectral Sensing or XRD, can quickly provide valuable information for grade control.

Future developments

Although the results of this study demonstrated that it is possible to reach good accuracy with the portable XRF for ore-waste and ore type classification, the application of ore classification systems on the results is not a straightforward process and still demands data to be exported and then processed manually. The development of software which could automatically apply ore classification systems on multiple analyses would increase the speed of the decision-making process. Additionally, the measurement of uncertainty related to portable XRF data could allow its integration into the deposit's database and its use in the modeling process, decreasing estimation errors (Narciso et al., 2019).

The automatic integration of portable XRF data with cloud-based platforms combined with the use of Machine Learning and Big Data creates the opportunity for an unprecedented optimization of stochastic models. This could lead to fast uncertainty reduction and, in turn, would require new decision-making approaches for mine planning, such as adaptive state-dependent policies (Paduraru and Dimitrakopoulos, 2018). This approach comprises a set of actions to be taken by mine operation and/or processing plant, which is updated in real time, based on new information collected by the portable XRF and uploaded into a cloud-based system (e.g., ore-waste classification).

CONCLUSIONS

Portable XRF can be successfully used for ore-waste and ore type classification of iron ores if correct calibration strategies are applied, in combination with appropriate sampling techniques and a QA/QC program. The immediacy of portable XRF analysis represents an opportunity to provide real-time information for grade control, instead of using traditional methods that can take days to make data available. This is particularly valuable for iron ore mines with high phosphorus zones.

However, some technical challenges still need to be addressed before this technology can be operational for

grade control, such as sample support validation and automation of information processing. Portable XRF can be of great value especially when combined with other analytical techniques that can identify minerals on a large scale, e.g., Hyperspectral Sensing or XRD.

ACKNOWLEDGMENTS

The authors are thankful to Vale S.A. for providing the samples, to REFLEX for providing access to the portable XRF and portable Press, and Marcela Tainá for the CRMs. The comments of the two reviewers — Carlos Spier and an anonymous one — are also appreciated by the authors.

REFERENCES

- Alkmin, F. F., Marshak, S. (1998). Transamazonian Orogeny in the Southern São Francisco Craton Region, Brazil: evidence for Paleoproterozoic collision and collapse in the Quadrilátero Ferrífero. *Precambrian Research*, 90(1-2), 29-58. [https://doi.org/10.1016/S0301-9268\(98\)00032-1](https://doi.org/10.1016/S0301-9268(98)00032-1)
- Andrade, F. R. D., Gobbo, L. A., Sousa, L. F. A. (2016). Iron ore classification by XRD-Rietveld and cluster analysis. *Geologia USP. Série Científica*, 16(2), 19-24. <https://doi.org/10.11606/issn.2316-9095.v16i2p19-24>
- Araújo, C. P., Costa, J. F. L., Koppe, V. C. (2018). Improving short-term grade block models: alternative for correcting soft data. *REM, International Engineering Journal*, 71(1), 117-122. <http://dx.doi.org/10.1590/0370-44672016710007>
- Beretta, F., Rodrigues, A. L., Peroni, R. L., Costa J. F. C. L. (2019). Automated lithological classification using UAV and machine learning on an open cast mine. *Applied Earth Science*, 128(3), 79-88. <https://doi.org/10.1080/25726838.2019.1578031>
- Blom, M., Pearce, A., Stuckey, P. (2019). Short-Term Planning for Open Pit Mines: A Review. *International Journal of Mining Reclamation and Environment*, 33(5), 318-339. <https://doi.org/10.1080/17480930.2018.1448248>
- Costa, A. G., Costa, F. J., Bonfioli, L. E., Rodrigues, M. L. (2001). Geologia de Mina na Samarco Mineração: um Suporte ao Planejamento de Curto Prazo / Controle de Qualidade, com Ênfase no Controle Mineralógico e na Previsibilidade do Comportamento dos Tipos de Minério no Processo. *III Simpósio Brasileiro de Minério de Ferro*. Ouro Preto: ABM.
- Dalm, M., Buxton, N., Ruitenbeek, A. (2017). Discriminating ore and waste in a porphyry copper deposit using short-wavelength infrared (SWIR) hyperspectral imagery. *Minerals Engineering*, 105, 10-18. <https://doi.org/10.1016/j.mineng.2016.12.013>
- Engström, K., Esbensen, K. (2017). Optimal grade control sampling practice in open-pit mining - a full-scale blast hole versus reverse circulation variographic experiment. *Applied Earth Science*, 126(4), 176-187. <https://doi.org/10.1080/03717453.2017.1414104>
- Farina, F., Albert, C., Martínez Dopico, C., Aguilar Gil, C., Moreira, H., Hippertt, J. P., Cutts, K., Alkmin, F. F., Lana, C. (2016). The Archean-Paleoproterozoic evolution of the Quadrilátero Ferrífero (Brazil): Current models and open questions. *Journal of South America Earth Sciences*, 68, 4-21. <https://doi.org/10.1016/j.jsames.2015.10.015>
- Fernandes, E. Z. (2008). *Caracterização Física, Química, Mineralógica e Metalúrgica dos Produtos Granulados de Minério de Ferro*. Thesis (Doctorate). Belo Horizonte: Escola de Engenharia, Universidade Federal de Minas Gerais.
- Fraser, J., Whitbourn, L., Yang, K., Ramanaidou, E., Connor, P., Poropat, G., Soole, P., Mason, P., Coward, D., Phillips, R. (2006). Mineralogical Face-Mapping Using Hyperspectral Scanning for Mine Mapping and Control. *6th International Mining Geology Conference*. Darwin: AUSIMM.
- Gazley, M. F., Duclaux, G., Fischer, L. A., Tutt, C. M., Lathan, A. R., Hough, R. M., De Beer, S. J., Taylor, M. D. (2015). A comprehensive approach to understanding ore deposits using portable X-ray fluorescence (pXRF) data at the Plutonic Gold Mine, Western Australia. *Geochemistry: Exploration, Environment, Analysis*, 15(2-3), 113-124. <https://doi.org/10.1144/geochem2014-280>
- Gazley, M. F., Tutt, C. M., Fischer, L. A., Lathan, A. R., Duclaux, G., Taylor, M., de Beer, S. (2014). Objective geological logging using portable XRF geochemical multi-element data at Plutonic Gold Mine, Marymia Inlier, Western Australia. *Journal of Geochemical Exploration*, 143, 74-83. <https://doi.org/10.1016/j.gexplo.2014.03.019>
- Hawke, P. J., Bachmann, J. (2018). A new blasthole XRF probe for mining grade control. *ASEG Extended Abstracts*, 2018(1), 1-5. https://doi.org/10.1071/ASEG2018abT7_1D
- Lessard, J., de Bakker, J., McHugh, L. (2014). Development of ore sorting and its impact on mineral processing economics. *Minerals Engineering*, 65, 88-97. <https://doi.org/10.1016/j.mineng.2014.05.019>

- Narciso, J., Araújo, C. P., Azevedo, L., Nunes, R., Costa, J. F., Soares, A. (2019). A Geostatistical Simulation of a Mineral Deposit using Uncertain Experimental Data. *Minerals*, 9(4), 247. <https://doi.org/10.3390/min9040247>
- Nayak, P., Hitch, M., Bamber, A. (2017). Increasing the value of heterogeneous ore deposits by high-resolution deposit-modelling and flexible extraction techniques. *Mining Technology*, 126(3), 139-150. <https://doi.org/10.1080/14749009.2016.1263008>
- Ortiz, C. E. A. (2014). *Caracterização Geometalúrgica e Modelagem Geoestatística da Mina de Brucutu - Quadrilátero Ferrífero (MG)*. Thesis (Doctorate). Ouro Preto: Escola de Minas, Universidade Federal de Ouro Preto.
- Paduraru, C., Dimitrakopoulos, R. (2018). Adaptive policies for short-term material flow optimization in a mining complex. *Mining Technology*, 127(1), 56-63. <https://doi.org/10.1080/14749009.2017.1341142>
- Parian, M., Lamberg, P., Möckel, R., Rosenkranz, J. (2015). Analysis of mineral grades for geometallurgy: Combined element-to-mineral conversion and quantitative X-ray diffraction. *Minerals Engineering*, 82, 25-35. <http://dx.doi.org/10.1016/j.mineng.2015.04.023>
- Pereira, A. C., Papini, R. M. (2015). Processes for phosphorus removal from iron ore - a review. *REM, International Engineering Journal*, 68(3), 331-335. <http://dx.doi.org/10.1590/0370-44672014680202>
- Ramanaidou, E., Wells, M. (2011). Hyperspectral Imaging of Iron Ores. *10th International Congress for Applied Mineralogy*. Trondheim: ICAM.
- Rosière, C., Spier, C., Rios, F., Suckau, V. (2008). The Itabirites of the Quadrilátero Ferrífero and Related High-Grade Iron Ore Deposits: An Overview. *Economic Geology*, 15, 223-254. <https://doi.org/10.5382/Rev.15.09>
- Snowden, V. (1993). Comparative 3-D resource modeling approaches at Macraes deposit in New Zealand and their reconciliation with production. *Applications of Computers in the Mineral Industry*. New South Wales: University of Wollongong, p. 42-45.
- Spangenberg, I. C., Minnit, R. C. (2014). An overview of sampling best practice in African mining. *The Journal of the Southern African Institute of Mining and Metallurgy*, 114(1), 91-102.
- Stanley, C., Lawie, D. (2007). Average Relative Error in Geochemical Determinations: Clarification, Calculation, and a Plea for Consistency. *Exploration and Mining Geology*, 16(3-4), 265-274. <https://doi.org/10.2113/gsemg.16.3-4.267>
- Urbano, E. E. M. C. (2017). *Gênese do Jazigo de Ferro de Moncorvo e Avaliação do Uso de Equipamentos Portáteis de FRX e DRX para a Exploração Mineral deste Tipo de Jazigos*. Thesis (Doctorate). Vila Real: Escola de Ciências da Terra e da Vida / Universidade de Trás-os-Montes e Alto Douro.

Appendix 1. Analytical results and ore type classification with and without calibration factors for each sample.

Sample	Laboratory XRF		Portable XRF with NCF		Portable XRF with CF		Sample	Laboratory XRF		Portable XRF with NCF		Portable XRF with CF	
	Fe (%)	Ore Type	Fe (%)	Ore Type	Fe (%)	Ore Type		P (%)	Ore Type	P (%)	Ore Type	P (%)	Ore Type
1	19.75	Very Low	18.85	Very Low	17.35	Very Low	0.145	Intermediary	0.186	High	0.106	Intermediary	
2	21.19	Very Low	21.16	Very Low	19.46	Very Low	0.120	Intermediary	0.184	High	0.105	Intermediary	
3	29.75	Very Low	30.01	Low	27.61	Very Low	0.110	Intermediary	0.199	High	0.114	Intermediary	
4	35.06	Low	35.01	Low	32.21	Low	0.095	Low	0.137	Intermediary	0.079	Low	
5	36.73	Low	34.80	Low	32.02	Low	0.091	Low	0.152	High	0.087	Low	
6	36.85	Low	36.55	Low	33.63	Low	0.090	Low	0.122	Intermediary	0.070	Low	
7	37.53	Low	39.20	Low	36.07	Low	0.085	Low	0.145	Intermediary	0.083	Low	
8	37.81	Low	38.04	Low	35.00	Low	0.071	Low	0.136	Intermediary	0.078	Low	
9	38.37	Low	38.85	Low	35.74	Low	0.068	Low	0.123	Intermediary	0.070	Low	
10	39.24	Low	39.98	Low	36.79	Low	0.064	Low	0.120	Intermediary	0.069	Low	
11	40.38	Intermediary	41.80	Intermediary	38.46	Low	0.059	Low	0.092	Low	0.053	Low	
12	41.14	Intermediary	40.24	Intermediary	37.03	Low	0.059	Low	0.119	Intermediary	0.068	Low	
13	41.20	Intermediary	41.84	Intermediary	38.50	Low	0.051	Low	0.103	Intermediary	0.059	Low	
14	42.25	Intermediary	42.12	Intermediary	38.75	Low	0.035	Very Low	0.077	Low	0.044	Very Low	
15	44.42	Intermediary	43.85	Intermediary	40.35	Intermediary	0.032	Very Low	0.073	Low	0.042	Very Low	
16	45.99	Intermediary	47.22	Intermediary	43.45	Intermediary	0.031	Very Low	0.031	Very Low	0.018	Very Low	
17	46.12	Intermediary	47.31	Intermediary	43.53	Intermediary	0.030	Very Low	0.040	Very Low	0.023	Very Low	
18	47.43	Intermediary	47.08	Intermediary	43.32	Intermediary	0.030	Very Low	0.045	Very Low	0.026	Very Low	
19	53.32	High	56.85	High	52.31	High	0.028	Very Low	0.000	Very Low	0.000	Very Low	
20	54.04	High	55.94	High	51.47	High	0.025	Very Low	0.016	Very Low	0.009	Very Low	
21	58.90	High	61.10	Very High	56.22	High	0.024	Very Low	0.012	Very Low	0.007	Very Low	
22	59.97	High	62.72	Very High	57.71	High	0.023	Very Low	0.031	Very Low	0.018	Very Low	
23	60.65	Very High	62.81	Very High	57.79	High	0.018	Very Low	0.031	Very Low	0.018	Very Low	
24	64.67	Very High	67.03	Very High	61.68	Very High	0.015	Very Low	0.056	Low	0.032	Very Low	
25	66.51	Very High	69.14	Very High	63.62	Very High	0.014	Very Low	0.024	Very Low	0.013	Very Low	
Miss classification:				Miss classification:		Miss classification:							
		3		5				15				0	

*Ore type classification follows Table 1; XRF: X-ray fluorescence; NCF: no calibration factor; CF: calibration factor.